ingegneria sismica
International Journal of Earthquake Engineering
Anno XXXVI – Num.4 - 2019

POST-EARTHQUAKE DAMAGE ASSESSMENT OF MOMENT RESISTING STEEL FRAMES

Claudio Bernuzzi, Davide Rodigari, Marco Simoncelli

Department of Architecture, Built Environment and Construction Engineering
Politecnico di Milano, Italy

SUMMARY: *The assessment of damage in structures that have suffered one or more earthquakes is of paramount importance to better understand the post-earthquake effective behaviour, and eventually to define the more appropriate design strategies for retrofitting and repairing.*
The paper, which is focused on moment-resisting (MR) steel frames, deals with post-earthquake assessment after one or more seismic events. A procedure combining non-linear time-history finite element analysis with the low-cyclic fatigue theory have been applied to appraise the damage level of each frame component and then the residual load carrying capacity have been evaluated via the incremental static analysis of the damaged frames. It is worth underlining that, on the basis of the discussed numerical results, the damage measurement and the residual load carrying capacity, which are often neglected in routine design, appear very useful to increase the knowledge on the effective safety level of the frame after one or more earthquake.

KEYWORDS: *moment-resisting (MR) steel frames, non-linear time-history analysis (NLTH), low-cycle fatigue (LCF), cyclic joint behaviour, load carrying capacity.*

1 Introduction

A large number of seismic events have clearly demonstrated that steel structures represent an efficient solution for buildings. This is due to the basic properties of the material combined with the presence of suitable components, that can be properly designed to dissipate earthquake energy (Figure 1) [Gioncu and Mazzolani, 2014].
Most recent design codes (like the EN1998, [CEN, 2004]), that are based on the well-known Performance Based Design approach, provide very useful information to structural engineers on how guarantee the required target performances (TPs) for prefixed levels of seismic risk. Making reference to the TP of "Life Safety", that is usually assumed as a key reference in the design phase, it is generally satisfied by admitting a limited damage of the structure and by preventing brittle collapses [Piluso *et al.*, 2019].
Nevertheless, Northridge and Kobe earthquakes [Youseff *et al.*, 1995] have clearly shown that damage in steel connections could produce economic loss significantly beyond any expectation [Mahin S.A., 1998, Dell'Aglio *et al.*, 2017, Montuori *et al.*, 2015].

Corresponding author: Marco Simoncelli, Politecnico di Milano, Italy.
Email: marco.simoncelli@polimi.it

Figure 1 - *Global deformation of MR- steel frame after an earthquake [Gioncu and Mazzolani, 2014]*

Investigations and repair activities constitute a relevant part of the total economic loss associated with earthquake, whose reduction depends on the ability of the engineers to find rapid and efficient design strategies. As a consequence, suitable approaches should be available for designers to allow for a compromise between the definition of adequate safety levels and the limitation of the economic loss. Furthermore, results of some experimental activities [Kato *et al.*, 1997] showed that the quite modest resistance to fatigue is in many cases due to the low material toughness, poor welding performance, strain rate effects and low temperature effects.

The traditional approaches, based on linear seismic analyses [Bernuzzi *et al.*, 2018] plus member verification checks, according to the same equations used for the monotonic load design [Bernuzzi *et al.*, 2015], cannot give any information about the damage in the key components. Moreover, these methods are not able to account accurately for the deterioration mechanisms experienced in the dissipative zone during earthquakes and for the relevant second order effects typically associated to the behaviour of steel structures [Tartaglia *et al.*, 2018; Dell'aglio *et al.*, 2019]. These aspects cannot be neglected when the considered dissipative zones are remarkably influenced by pinching and strength/stiffness drops under cyclic loads (Figure 2), as in semi-rigid steel joints [Ferraioli *et al.*, 2018].

In the European seismic design code of steel frames (EN1998 [CEN, 2004]), fatigue checks are not required, that could be of great interest to appraise the residual life of frames, being code attention addressed only on the ductility and resistance of the components. It is only prescribed to perform *in-situ* visual inspection directly on the deformed structure. Unfortunately, from the practical point of view, inspections are often difficult because of the presence of non-structural elements hampering the identification of damages in members and connections. Therefore, it appears essential in the assessment of the residual performance of a damaged structure, the application of advanced numerical methods allowing also for predicting the damage location as well as its amount.

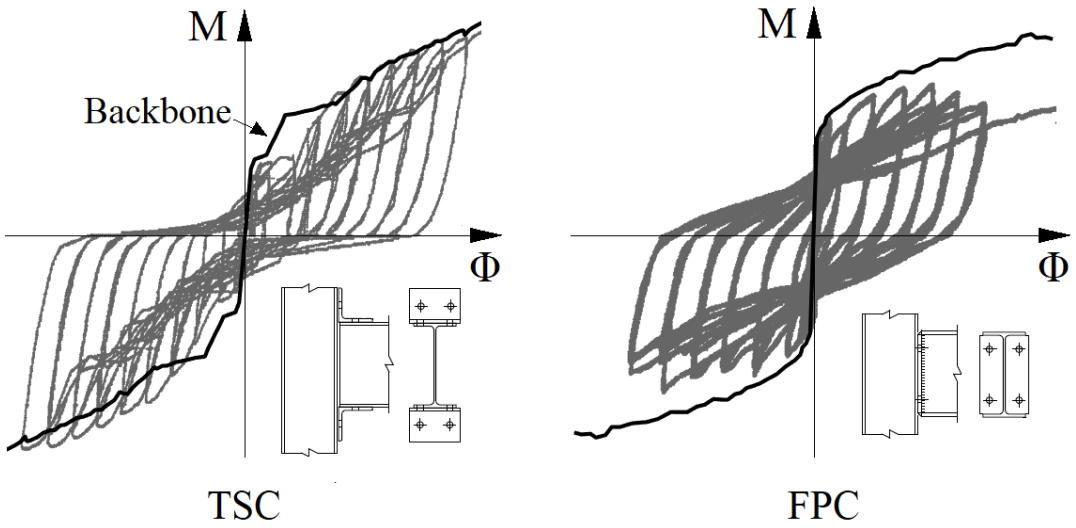

Figure 2 - *Moment (M) – Rotation (Φ) behaviour of semi-rigid steel joints [Bernuzzi et al.,1996]*

Only few researches have been addressed to the damage appraisal after an earthquake. In particular, the reliability of Moment Resisting (MR) steel frame components after an earthquake has been suitably investigated by extending high-cyclic fatigue theory [Ballio *et al.*, 1997, Vayas *et al.*, 2003]. A refined approach has already been proposed for steel storage racks [Bernuzzi and Simoncelli, 2016], combining non-linear time-history (NLTH) analyses and the low-cyclic fatigue (LCF) theory. In these cases, frame components were in class 4, according to EN1993-1-1 [CEN, 2005] classification criteria, and non-linearities were accounted for only in beam-to-column and base-plate joints. A similar procedure has been herein extended to traditional carpentry frames, whose components are in class 1, i.e. interested by the spread of plasticity along the cross-section and the whole member. In particular, this paper discusses key results of the procedure applied to two MR steel frames differing for connections, focusing mainly on the measurement of the damage level and on the post-earthquake residual load carrying capacity.

2 Remarks on the actual post-earthquake assessment procedures

The post-earthquake damage assessment is a multi-step process aimed at mapping the damage location in buildings, that is a necessary pre-requisite to predict the residual level of safety against future loading conditions and, when necessary, to define repair actions or the need to demolish the building. Inspections are often necessary for the identification of critical situations and for defining the hazard level associated with the damaged structures. Several indications about residual performance of MR frames have already been provided by USA standards, developed after the Northridge earthquake in the framework of the FEMA/SAC Steel research Program [FEMA 352, 2000]. Post-earthquake damage assessment is carried out in two phases:

- *Preliminary Evaluation*: a general inspection of the building allows for a qualitative evaluation of the key parameters directly associated with the safety of the structure, like residual interstorey drift and structural and non-structural damages. The main scope of this phase is to provide a rapid definition of a rating about the building condition, in

general classified as: minor damaged (habitable after detailed evaluation), damaged (habitable after repair actions) or unsafe (to be demolished).

- *Detailed Evaluation*: this process is applied to building classified as damaged. Its scope is to determine the impact of the detected damage on the residual performance of the structure. A judgment about the structural safety and the design of the repairs is based on the quantitative definition of the damage levels: *Level 1* and *Level 2*.
  In *Level 1*, the evaluation is based on a deep inside inspection considering all or some selected components for estimating the global damage level of the building. A suitable damage index d_j is defined for the inspected connection combining each single damage mode detected in beam, joint and column according to specific tables [FEMA 352, 2000]. In Figure 3, as an example the indices related to beam damages are reported.

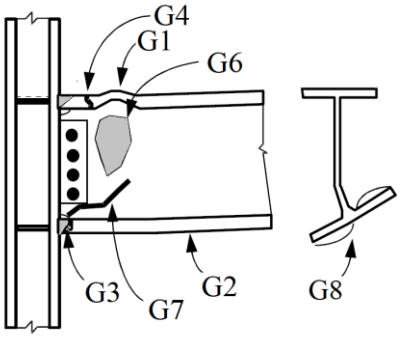

Type		Description	Index
SINGLE	G1	Buckled flange (top or bottom)	2
	G2	Yielded flange (top or bottom)	0
	G3	Flange fracture in Heat Affected Zone (top or bottom)	2
	G4	Flange fracture outside Heat Affected Zone (top or bottom)	2
	G6	Yielding or buckling of web	2
	G7	Fracture of web	4
	G8	Lateral torsion buckling of section	2

	Combination	d_j
COMBINED	G1+G2	2
	G1+G3	4

Figure 3 – *Type of beam damage and related index [FEMA 352, 2000]*

Then damage indices are grouped by floor and the whole damage index at *i-th* floor (D_i), is obtained as:

$$D_i = \frac{1}{n_c} \sum_{j=1}^{n_c} \frac{d_j}{4} \tag{1}$$

where n_c is the number of damaged connections in the considered floor group and d_j is the associated damage index.

The maximum floor damage D_{max} for the building is the maximum values of D_i in the considered frame. As a general criterion all the connections with a damage index d_j higher than 1 must be repaired. Moreover, if the maximum floor damage is greater than 0.5 a more accurate *Level 2* evaluation must be performed.

In case of *Level 2*, the inspections are conducted on all the critical structural elements and a numerical model has to be used accounting for strength and stiffness reduction in the damaged state. The final scope is to evaluate the residual resistance of the structure. Once selected the method and performed the analysis, several approaches can be applied in supporting the decision-making process. For example, it can be done by considering the capacity of building related to the pre-earthquake load carrying capacity. Generally, it is accepted a residual capacity of 90% with no repairs. Otherwise, if the residual capacity is lower than 50% the structural performance should be significantly cut down.

Another parameter that is used to define the damage state of buildings is the interstorey drift. Two drift types are considered: the maximum value of the admitted residual drift ($\theta_{r,max}$) and the admitted transient drift ($\theta_{t,max}$), that is the maximum drift reached during the earthquake. The admitted values are reported in Table 1.

Table 1 –Damage state from maximum residual ($\theta_{r,max}$) and transient drift ($\theta_{t,max}$) [FEMA, 2018]

Structural Damage State	Description	$\theta_{r,max}$ (mrad)	$\theta_{t,max}$ (mrad)
No Structural Damage	Repair of nonstructural component, residual drift equal to the maximum construction tolerance of new buildings	2	15
Slight Damage	Realignment of structural frame and structural repair are required to maintain permissible drift limits for non-structural component and limit degradation in structural stability	5	27
Moderate Damage	Major structural realignment is required to restore margin of safety for lateral stability; however, repair may not be economically and practically feasible	10	41
Heavy Damage	Residual drift very large that structure is danger of collapse from earthquake aftershocks	30*	71

*value taken from [Ohi and Takanashi, 1998]

Residual drifts describe the permanent deformations of the structure and can be directly evaluated on the frame also in presence of claddings and partitions. Otherwise, maximum transient drift distribution can be estimated by simplified approaches or by more refined structural analyses. Damage classification drift based allows for a direct evaluation, however no information are provided about the residual properties as well as about the damage level of the structural elements. Therefore, further investigations on the residual properties are needed to obtain an accurate estimation of building safety.
European guideline gives only instructions for a preliminary evaluation of seismic damage [Baggio *et al.*, 2007]. However, no specific procedures are provided for a detailed evaluation of the practical effects due to the earthquake and, in particular:

- *damage in each critical component (members and connections);*
- *residual and maximum interstory drift;*
- *effective performance;*
- *structural safety against future strong earthquakes.*

3 The proposed procedure

Basing on the previous remarks, the only approach that could conveniently be adopted for designing safely and optimally steel frames is the one based on non-linear time-history (NLTH) analyses [Clough and Penzien, 2003], suitably improved, to account for low-cycle fatigue (LCF) effects and, as a consequence, for the reduction of structural performance. More in detail, it seems convenient to make reference to the fatigue failure prediction via the well-established Whöler's approach for high-cycle fatigue [Bannantine *et al.*, 1989], that has already been extensively tested and validated for low-cycle fatigue [Ballio *et al.*, 1997, Krawinkler and Zohrei, 1983].
In particular, reference is made to the Bernuzzi *et al.* [1997] application for LCF analysis of semi-rigid joints and components. Transition between the safe and unsafe zones (Figure 4) is expressed as:

$$N(\Delta\Phi)^3 = K \tag{2}$$

Term N is the number of cycles to reach failure at the constant rotation range $\Delta\Phi$, the slope of the line distinguishing safe and unsafe regions is generally fixed to 3 [EN1993-1-9, 2009] in a

log-log scale and K is a constant depending on both component details and material properties [Ballio *et al.*, 1997].
This criterion allows for the evaluation of the fatigue failure of the component of interest only if subjected to constant amplitude loading history. With random loads, that are the ones associated with earthquakes, instead of $\Delta\Phi$ an effective equivalent rotation range value, $\Delta\Phi_{eq}$, has to be adopted, which is related to an equivalent constant loading history characterized by the same number of cycles (N) leading to the same damage. Term $\Delta\Phi_{eq}$ is defined as:

$$\Delta\Phi_{eq} = \left[\frac{1}{N}\sum_{i=1}^{n}\Delta\Phi_i^{\,3}\right]^{\frac{1}{3}} \tag{3}$$

where $\Delta\Phi_i$ is the total rotation range of each cycle of the variable amplitude loading history.
As to the cycle counting methods, i.e. the approaches to evaluate $\Delta\Phi_{eq}$, reference can be made to the *rainflow* procedure which is recommended by the European fatigue design code EN 1993-1-9 [CEN, 2009]. Furthermore, it should be of great interest, for practical design purposes, to measure the damage associated with each earthquake and/or with a set of subsequent seismic events. The so-called Miner's rule [Miner, 1945] could be conveniently applied also to frame components, making reference to the damage index D, which ranges from 0 (no damage) to 1 (failure for LCF), expressed as:

$$D = \frac{N \cdot \Delta\Phi_{eq}^{\,3}}{K} \tag{4a}$$

Rewriting Equation (4a) in log-log domain as in Equation (4b), once fixed the damage index D equal to an intermediate value D^* it is possible to obtain the so called iso-damage curves (Figure 4).

$$\log(N) + 3\log(\Delta\Phi_{eq}) = \log(K) + \log(D^*) \tag{4b}$$

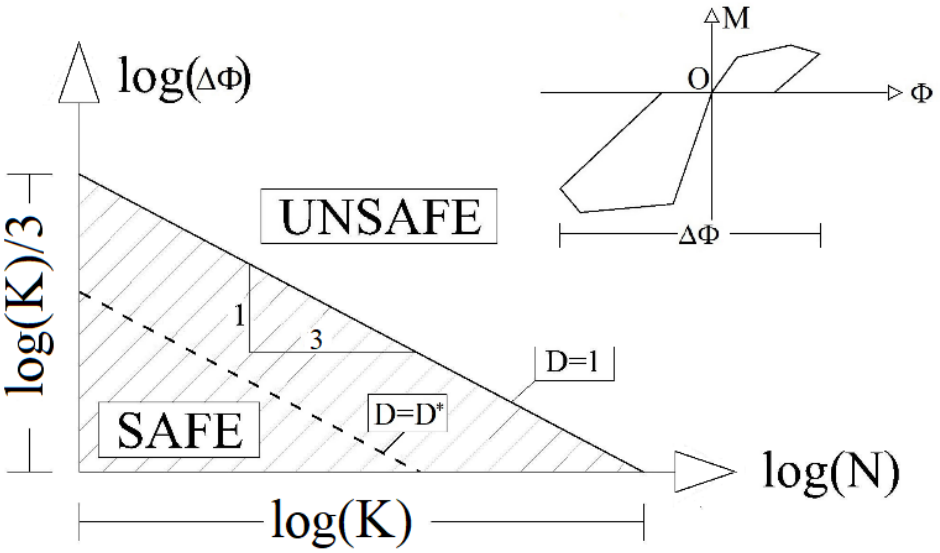

Figure 4 - *Fatigue resistance line in log(ΔΦ)-log(N) space*

After the modelling phase of the steel frame defining the geometric and mechanical properties of all the key components, for each accelerogram, the proposed procedure (Figure 5) is comprised of the following steps:

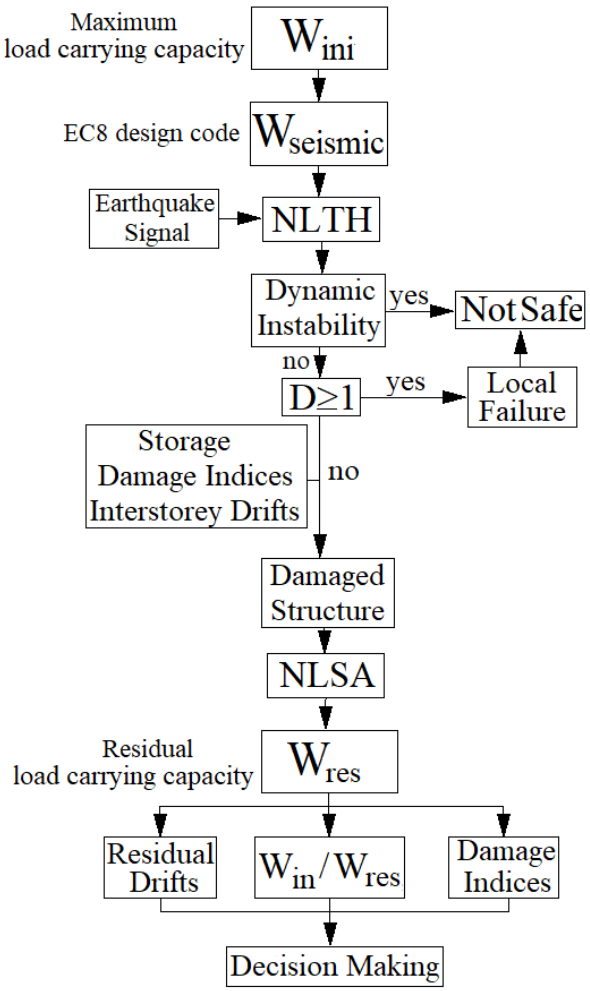

Figure 5 - *Flow-chart of the numerical procedure*

I. appraisal of the initial maximum monotonic load carrying capacity (W_{ini}) by means of Non-Linear Static Analysis (NLSA), incrementing the vertical loads;
II. execution of the NLTH analyses considering, according to EC8 [EN 1998-1, 2004], the seismic loading condition ($W_{seismic}$), taking into account both geometrical and mechanical non-linearities;
III. basing on the output data, evaluation of the damage index (D) for each component via the LCF design approach. Evaluation of the maximum and residual interstorey drift;
IV. evaluation of the residual load carry capacity performing a NLSA on the damaged structure (W_{res}), i.e. by taking into account the actual reduced behaviour parameter of the component;
V. definition of the most appropriate retrofitting strategy on the basis of the obtained results (previous steps).

4 The numerical study

The proposed approach is applied to two planar MR frames differing for the beam-to-column joint typology. As it appears from Figure 6, beams and columns are standard hot rolled IPE300 and HEA220 profiles, respectively. These components are connected to each other via steel details able to guarantee a typically semi-rigid behaviour, which has been experimentally investigated under cyclic loads [Bernuzzi *et al.*, 1996]. More in detail, the first considered beam-to-column connection is a top and seat angle (TSC), and the second one is a flush end plate connection (FPC).

The considered seismic mass is approximately 32 tons per floor. To reduce the number of variables affecting research outcomes, perfectly rigid connections are supposed at the bases. For the NLTH analysis, four earthquakes have been considered (Figure 7): El Centro 1979, Chi-Chi 1999, Northridge 1994 and Landers 1992 having the magnitude equal to 6.5, 7.6, 6.7 and 7.3, respectively. The first two El Centro (IMPVALL/H-DLT352) and Chi-Chi (CHICHI/TCU045-E) are far field record and the other two, Northridge (NORTHR/SYL090) and Landers (LANDERS/LCN_260), are near field signal. The records are available at the PEER Strong Motion Database [Chiou *et al.*, 2008].

Non-linear FE analyses have been carried out by means of OpenSees software [McKenna, 2011], each member have been discretized by ten beam element, including both geometrical and mechanical non-linearities; the former by using a corotational formulation [Denavit and Hajjar, 2013] and the latter accounted for a lumped plasticity approach. A non-linear rotational spring is considered attached to each beam end to simulate joint behaviour, accounting for the cyclic deterioration mechanisms experimentally appraised [Bernuzzi *et al.*, 1996], as depicted in Figure 8, in terms of both moment-rotation (M-Φ) law and energy dissipation.

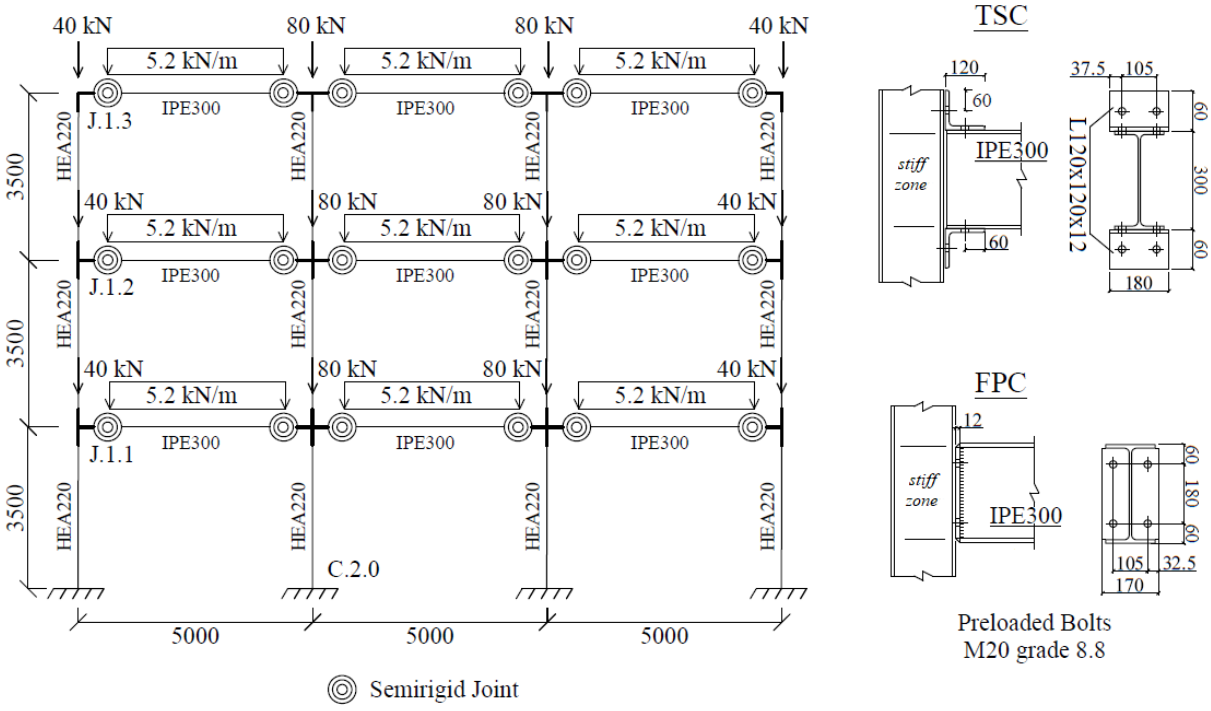

Figure 6 - *Frame configuration and load in seismic condition (dimensions are in millimetres)*

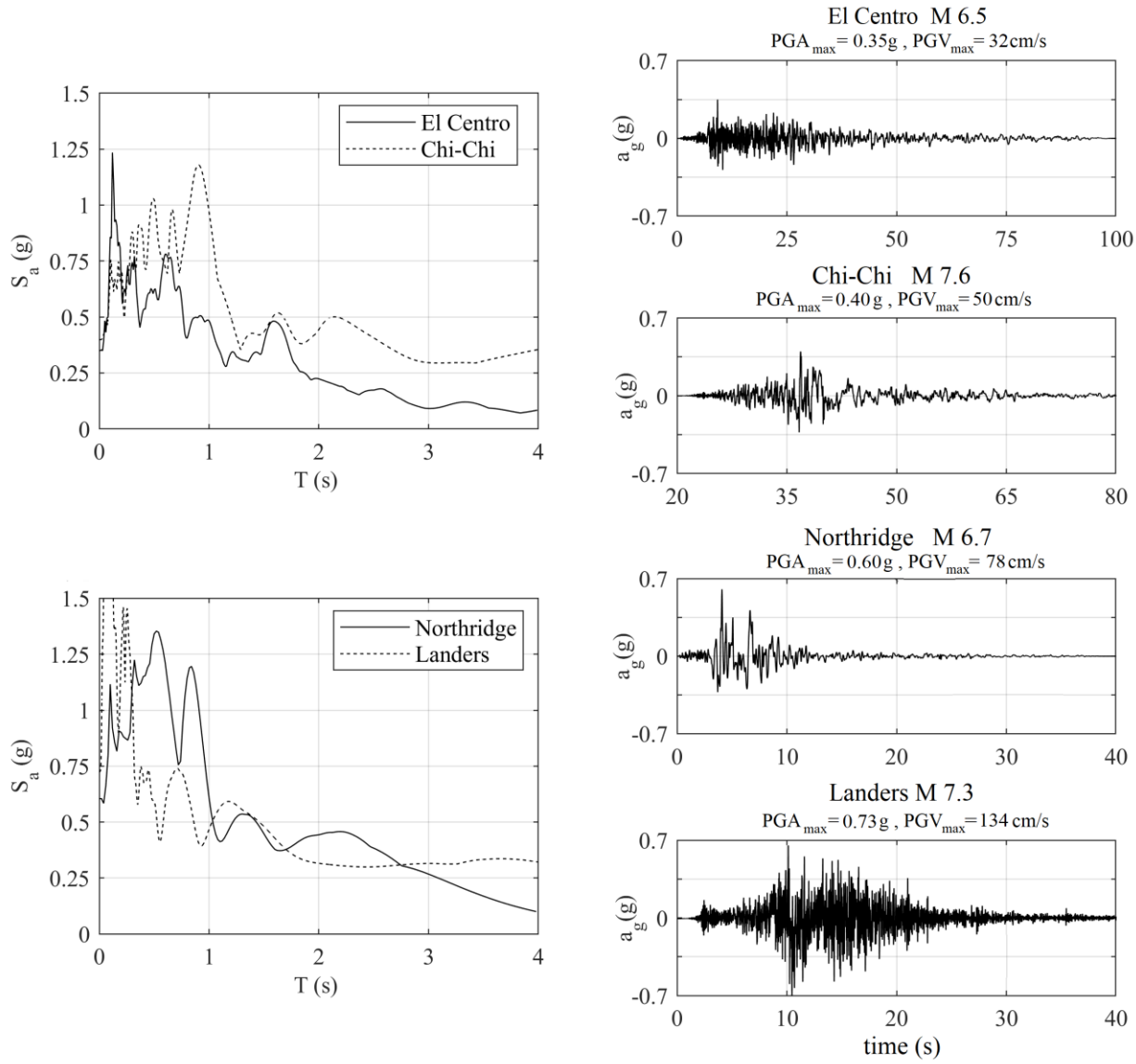

Figure 7 – *The considered Signals*

As to the ends of each column and the midspan of each beam, a bilinear moment-curvature relationship has been adopted with the possibility to define suitable cyclic responses, which have been calibrated on the basis of experimental tests [Ballio *et al.*, 1997]. More details about the calibration of the cyclic behaviour, can be found in ref. [Rodigari, 2020].
Elastic buckling analyses, which are of paramount importance for both static and seismic design, have been carried out and the load multiplier associated with the sole gravity loads in seismic combination, is 21.67 and 23.64 for TSC and FPC frame, respectively. As to the modal properties, the first (T_1) and the second (T_2) vibration modes are equal to 1.16s and 0.35s for TSC and 1.10s and 0.34s for the FPC, respectively. The mass participation is 86% for the first mode and 11% for the second, in both TSC and FPC frame. Damping matrix has been defined proportionally to the initial elastic stiffness matrix, as indicated in ref. [Zereian and Medina, 2010].

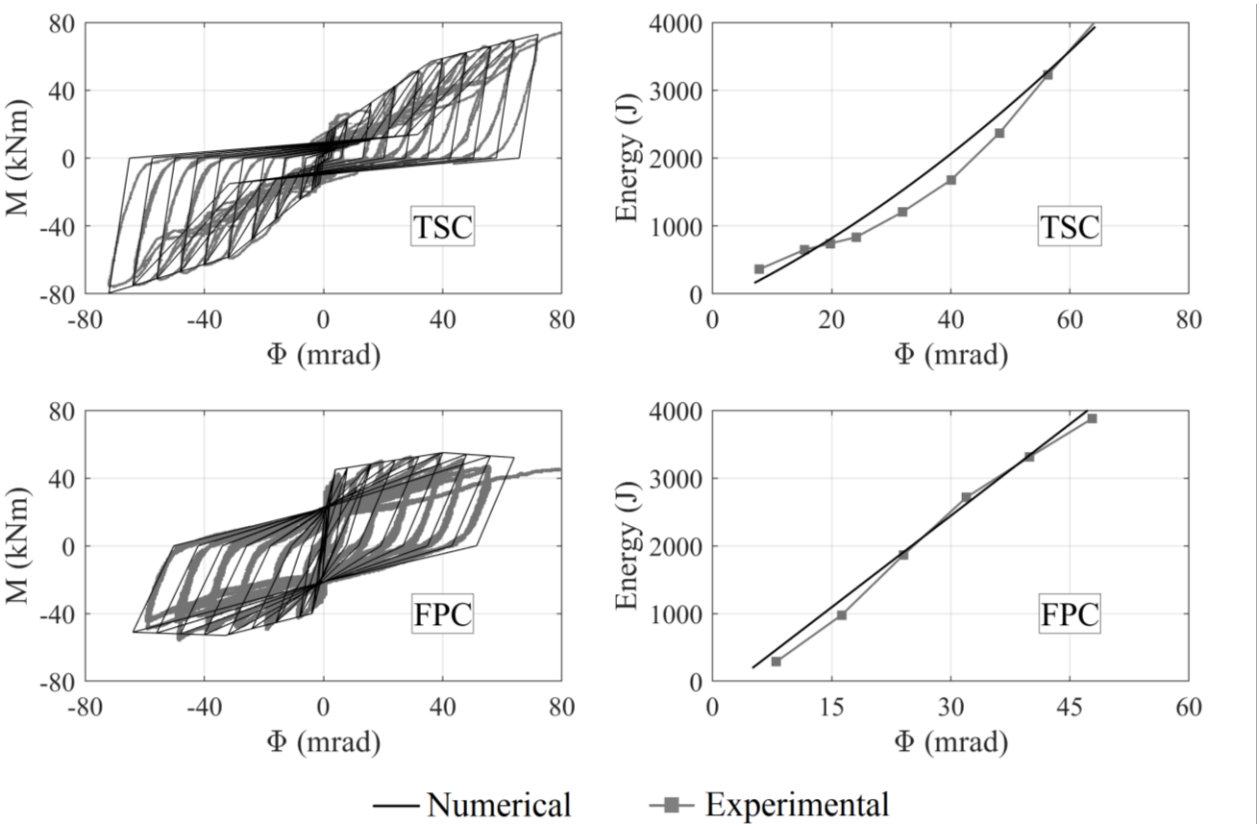

Figure 8 - *Calibration of the joint cyclic response.*

5 Earthquakes effects

As to the output results, at first attention has been focused on the joint behaviour and Figure 9 plots, as an example, the cyclic moment-rotation curves for J.1.2 beam-to-column joint due to all the considered earthquakes. In the same figure, also the curves of the column end C.2.0 cross-sections are presented but only for the most two severe earthquakes, suffering these cross-sections of very limited excursions in plastic range with cycles limited in number and amplitude. It can be noted that TSC joints provide maximum rotation values similar to FPC, with the only exception of El Centro earthquake. In this case, the maximum joint rotation of TSC frame is approximately half of the one obtained in FPC frame. A great number of cycles have been observed with a quite small rotation amplitude range (lower than 5 mrad).

In order to appraise the damage values according to the previously described procedures, the well-established *rainflow* counting process has been adopted [ASTM, 2017] for each joint and member cross-section of interest. As an example of the associated results, Figure 10 can be observed where the rotation amplitudes ($\Delta\Phi$) and the related number of cycles are reported for the joint J.2.1, excluding cycles with an amplitude lower than 1 mrad, because negligible for the fatigue damage assessment. It can be noted that El Centro signal leads to a joint response characterized by high number of cycles with low amplitudes, for both FPC and TSC frames. Chi-Chi signal leads to a general widespread behaviour, with highest values of cycles at low amplitudes for FPC frame only. Finally, the other two signals are characterized by widespread behaviour showing, in general, a quite limited number of cycles, with the only exception of Northridge signal for FPC frame.

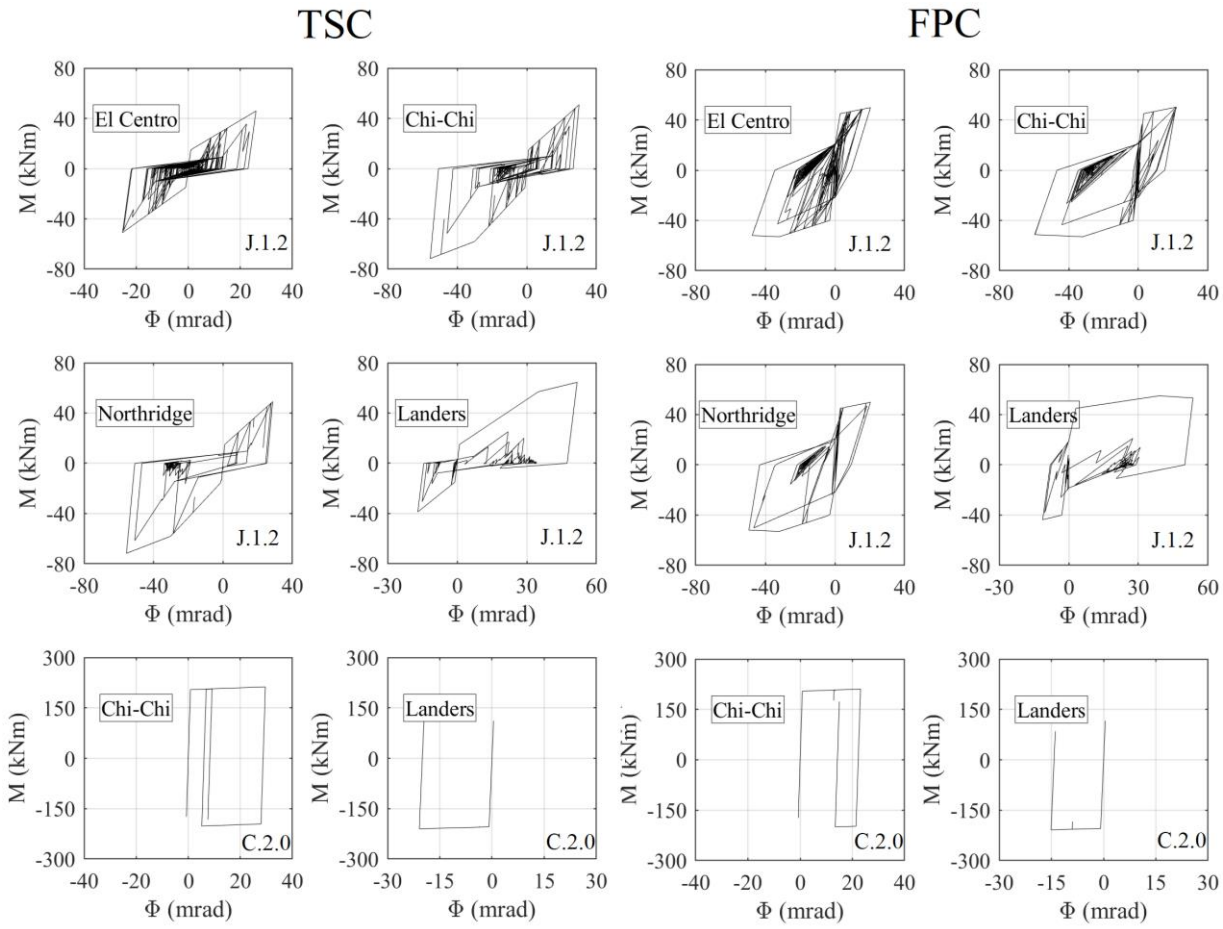

Figure 9 - *Hinge response of Joint J.1.2 and column base C.2.0*

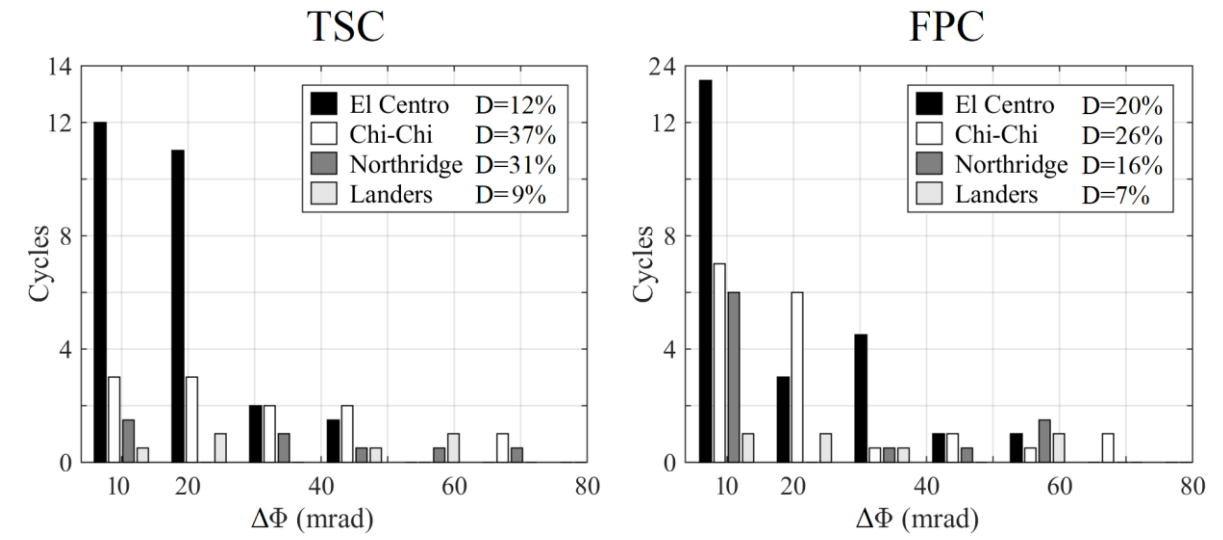

Figure 10 - *Rainflow counting Cycle of Joint J.1.2*

More in detail, the damage index for the considered J.2.1 joint associated with El Centro signal, assumes a non-negligible value of 12% and 20% for TSC and FPC, respectively. The

maximum damage is obtained in TSC model under Chi-Chi earthquake (D=37%), because of the great number of cycles in the rotation range between 30 and 70 mrad.
A more detailed damage assessment of both the frames is depicted in Figure 11 where for the considered dissipative zones, all the damage index values are reported for both joints and column ends in percentage. Moreover, a refined representation of joints fatigue is also proposed in the log-log Whöler's plane, making reference to the equivalent rotation ($\Delta\Phi_{eq}$) of Equation (3). In this reference system, the damage indices can be directly appraised by using the iso-damage lines (D^*), previously defined in Equation (4b).
Considering Figure 10, it can be noted that:

- in general, the damage of all the column end sections is negligible, except than for TSC frame under the Chi-Chi signal with damage values up to 21%;
- damage indices are non-negligible in the joints. Maximum are located at the second level and the minimum ones at the top. This is mainly due to the effects of the combination between the first and second vibration modes that have a maximum deformation demand at the middle height of the frame and minimum at the top;
- joints to external columns are always more damaged than the internal ones. For each beam, the damage indices at the joints have significant differences due to the presence of hogging moment due to gravity loads;
- the damage indices of joints related to internal beams are equal;
- El Centro is characterized by a greater number of cycles than the other accelerograms (more than three times).

The values of the damage indices of both TSC and FPC frames have been summarized for each earthquake in Table 2, in terms of mean value of the damage index for the bottom column ends, each floor and all floors together. It can be noted that the minimum and the maximum damages are obtained for Landers and Chi-Chi earthquake, respectively. Landers provides the lowest mean damage with a value of 3.5% for column base and 5.3% for joints in FPC frame. The highest mean damage index in Chi-Chi earthquake is equal to 19.5% for column bases and to 27.2% for joints, in TSC frame. If only Northridge and El Centro earthquakes are considered, the highest joint damage is observed in TSC during the former with a mean value of 20.2%, while the latter provides the highest value in column bases: 14.5% for FPC model. It can also be noted that TSC frame shows higher damage index in all the elements than the FPC one for all the considered earthquakes, with exception of the El Centro.

Table 2 – *Mean Joint damage index in percentage for each level and for the overall frames.*

Earthquake	Frame	*Column bases*	*Joints*			
			I floor	II floor	III floor	all floors
El Centro	TSC	6.5	9.4	11.5	6.9	9.3
	FPC	14.5	14.1	18.4	8.6	13.7
Chi-Chi	TSC	**19.5**	29.7	35.5	16.4	**27.2**
	FPC	13.0	19.0	24.7	11.3	18.3
Northridge	TSC	12.3	16.2	27.3	17.2	**20.2**
	FPC	6.5	10.2	15.7	5.6	10.5
Landers	TSC	4.5	6.0	9.2	5.6	6.9
	FPC	**3.5**	4.9	7.2	3.8	**5.3**

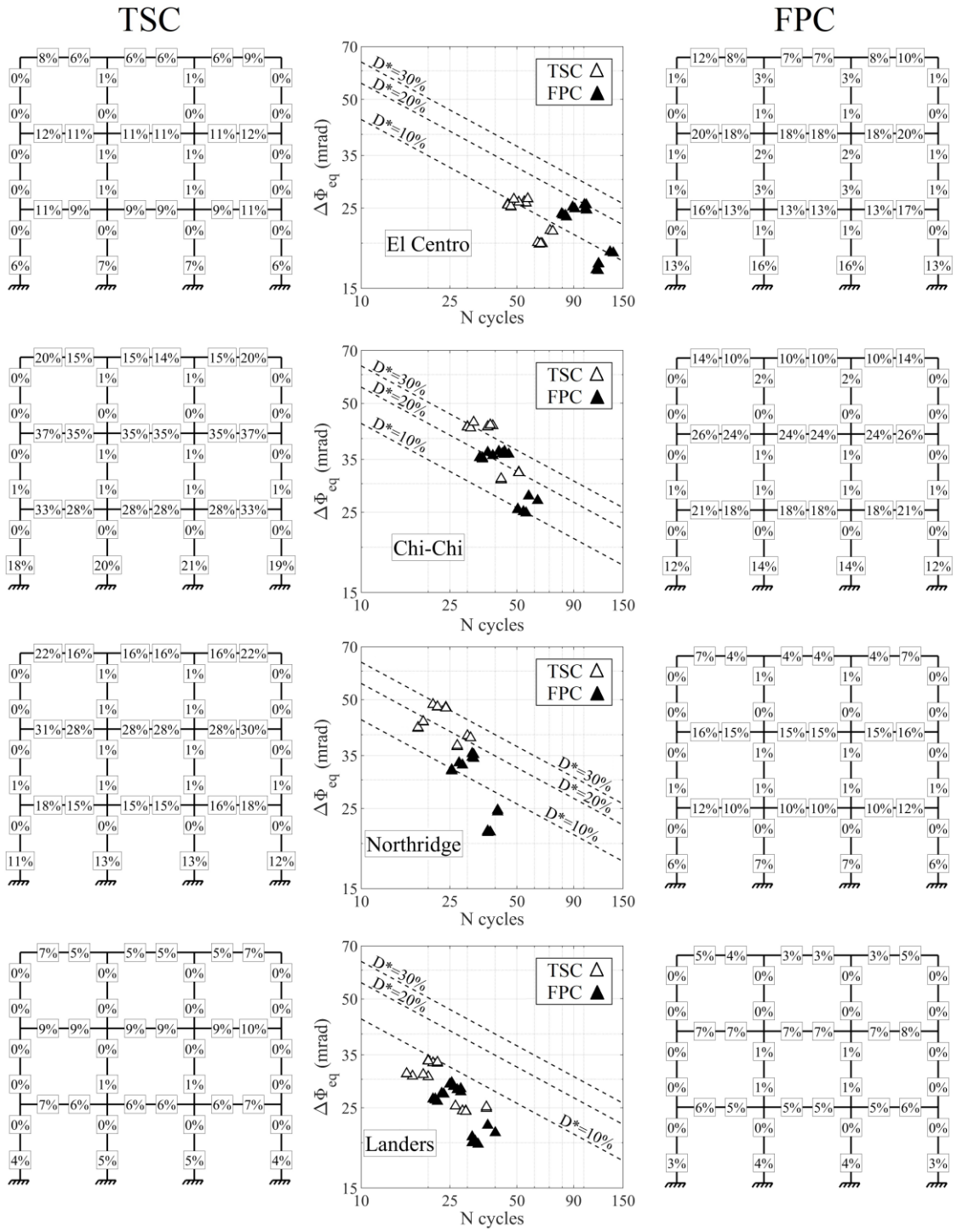

Figure 11 - *Local damage (%) distribution and Whöler's representation of semi-rigid joint damage*

Finally, it is worth noting that the proposed NLTH-LCF procedure allows for monitoring efficiently the damage evolution during the earthquake. As an example, Figure 12 can be considered, in which solid and dashed lines are related to the TSC and FPC frames, respectively and the relationship in term of damage (in percentage) versus time is proposed.

Due to the large amount of data, only the most highly damage joints with respect to each floor (i.e. J.1.1, J.1.2 and J.1.3) and column base sections (C.2.0) are considered.

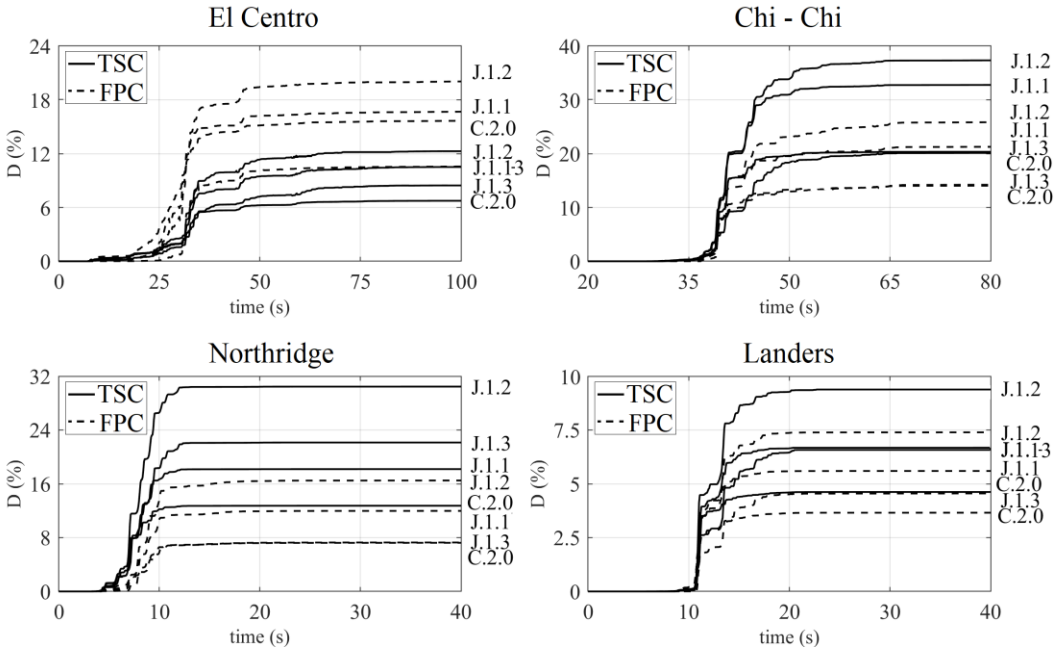

Figure 12 - *Damage cumulation (%) during the considered earthquakes*

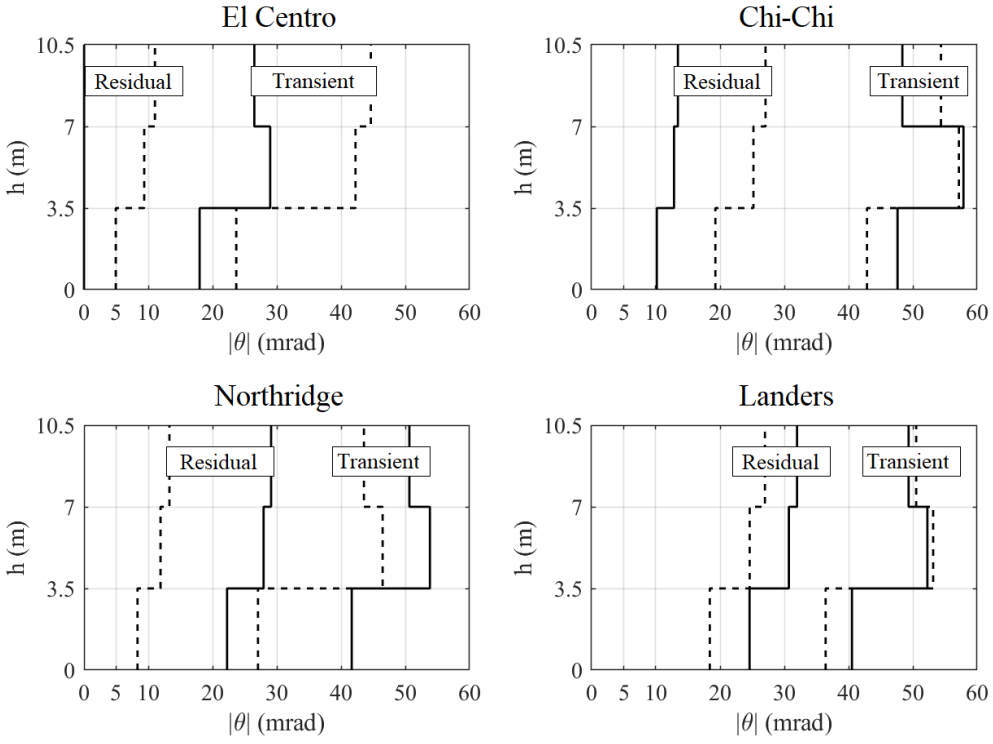

Figure 13 - *Residual and Maximum Transient drift distribution*

In near field signals (Northridge and Landers) the maximum damage is reached quite immediately unlike for far field signals (El Centro and Chi-Chi) where more than half of total earthquake duration is required.
Additional information on the building occupancy, structural and non-structural damage state and sustainability of repair actions can be obtained from the interstorey drift analysis. According to Table 1, attention has hence to be addressed to both residual and maximum transient drift. In Figure 13 the absolute values of residual and transient drifts, obtained from NLTH, are reported over the frame height, for both TSC and FPC frames.
It can be noted that highest transient drifts are always at the second floor, with the sole exception for FPC frame under El Centro Earthquake where the highest value is obtained at the top. The maximum and minimum values of transient drift are in the TSC frame during Chi-Chi and El Centro earthquakes, with a value of 58 mrad and 18 mrad, respectively. During events of stronger magnitude (Chi-Chi and Landers), transient drifts are quite similar for TSC and FPC frames unlike for El Centro and Northridge earthquakes, with a maximum scatter up to 40%. The residual drift increases from the base to the top in all the considered cases. The highest residual drift is obtained for TSC model in Landers earthquake, equal to 32 mrad. The lowest residual drift is equal to zero, detected for TSC frame under El Centro earthquake. Moreover, in near field signals, the residual drifts for TSC frame are, in general, higher than the one of FPC, with a maximum scatter up to 64% at the first floor, in case of Northridge earthquake. On the contrary, in far field signals, the highest residual drifts are showed in FPC model. By considering drift results and damage indices, it can be noted that the transient drift distribution is coherent with damage distribution along the frame height, being the maximum transient drifts at the second floor where the maximum damage has been observed. However, it cannot be defined a numerical correlation between damage and transient drift, as demonstrated by the fact that in Landers earthquake, quite important transient drifts are associated with low damage indices.
The other relevant aspect for the safe use of the frame after an earthquake is the evaluation of the residual load carrying capacity. Three are the key factors influencing the post-earthquake resources of a structure: i) the residual strength, ii) the residual stiffness and iii) the residual interstorey drifts. Those aspects have been directly accounted for in the structural model at the end of the NLTH analysis. The residual load carrying capacity has been evaluated via a NLSA. For the considered cases the vertical loads have been incremented monotonically up to collapse. Global imperfections were also accounted via a horizontal force at floor with a magnitude of 1/200 of the total floor weight. The obtained curves are represented in Figure 14 in terms of total vertical load (W_{tot}) versus the absolute value of lateral drift of the top of the structure ($|\theta_{top}|$). It can be noted that TSC frame presents a quite lower reduction of the carrying capacity after the earthquake than FPC frame. The highest residual capacity is obtained by TSC frame under El Centro earthquake: in this case the reduction of the initial capacity is very limited, lower than 4%. On the contrary, the maximum reduction is due to Chi-Chi earthquake for FPC frame, up to 39%. In the other cases the reduction with respect the initial load carrying capacity is up to 20%.
On the basis of the obtained results in terms of LCF damage indices, interstorey drift and residual load carrying capacity, it is possible to perform a post-earthquake evaluation of the structures. It can be concluded that, only for TSC frame subjected to El Centro earthquake, the structure can be assessed as slight damage (low damage level). In all the other cases, structure must be classified from moderate to heavy damage.

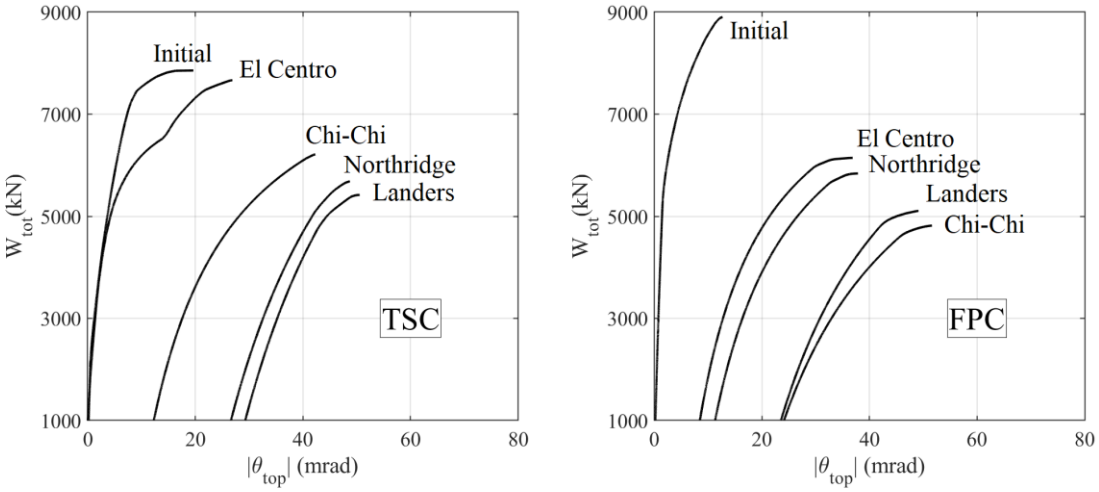

Figure 14 - *Residual Load carrying capacity assessment*

Finally, further information about the localization of repair activities and inspections can be obtained from the LCF damage distribution (Figure 10). These activities seem required only for the TSC frame under El Centro earthquake, while for the other cases, reparability cannot be considered economically sustainable due to the large amount of damages or of the residual drift.

6 Sequential Earthquakes effects

In the previous discussed results, no details are provided about the resistance of the structure against future seismic events. However, the evaluation of the residual seismic performance after more earthquake can be done by applying the same proposed assessment procedure. In this case, as discussed in literature [FEMA, 2000], it seems reasonable to consider that in a relative brief period, the seismic events that a region will experience have a similar magnitude of the original shock.

Therefore, the earthquake sequence for NLTH can be obtained as a repetition of the same main shock signal, previously described. A time interval with zero acceleration is needed between each repetition, allowing the stop of all the movements between an earthquake and another. Three repetitions of each earthquake have been herein considered. Due to relevant reduction in load carrying capacity obtained with a single earthquake, structural failure due to Dynamic Instability (DI) is expected [Bernal, 1992]. In fact, for the considered cases, DI occurs only in FPC model during the repetition of the largest magnitude earthquakes (Chi-Chi and Landers), as reported in Figure 15 were the top drift response (θ_{top}) is plotted versus the total time.

It can be noted that two different trends, in the drift cumulation process under sequential earthquakes, have been observed:

- progressive increment of residual and trasient drift, in FPC frame (with the exception of El Centro) and in TSC frame for Landers and Chi-Chi earthquakes;
- structural adaptation of the frame to the deformed shape after the first earthquake, that can be directly appreciated via Figure 15 from the total drift trace of FPC model under El centro earthquake.

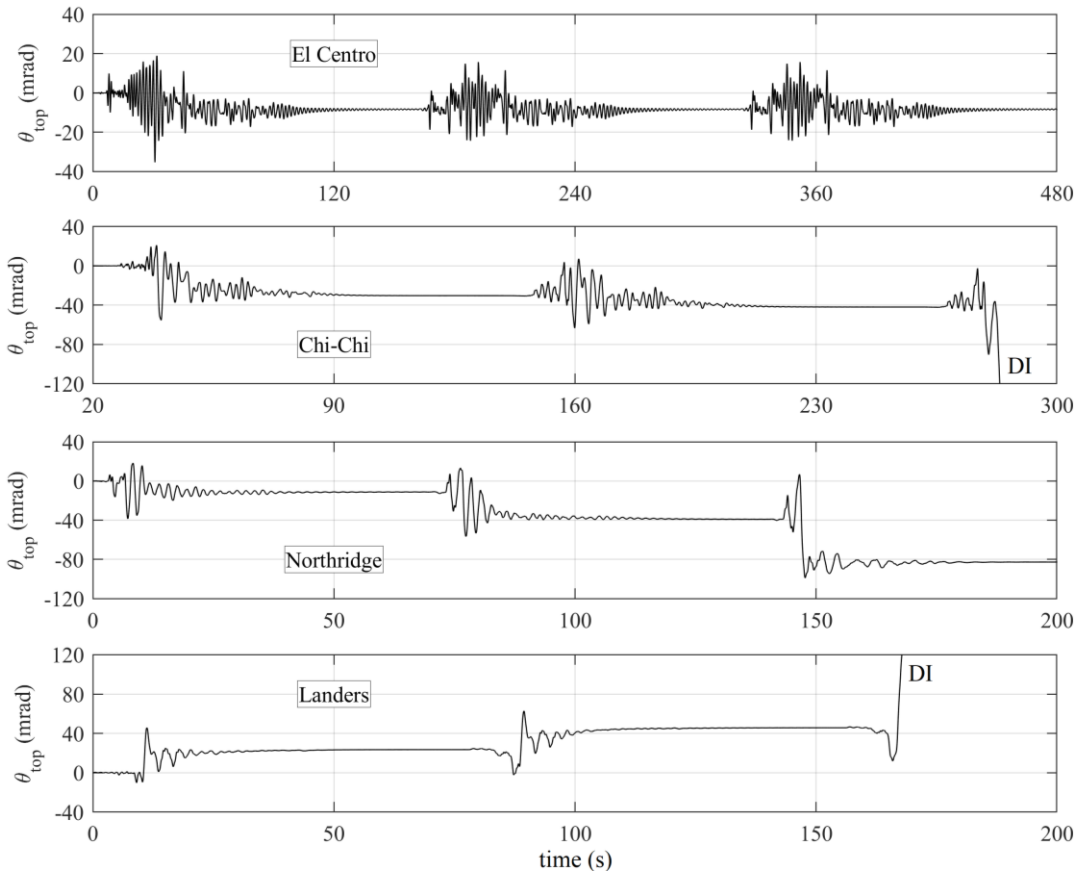

Figure 15 - *Top drift (θ_{top}) response of FPC frame*

An aspect of paramount importance is the evaluation of the residual load carrying capacity after each repetition. In Figure 16 the ratio between residual (W_{res}) and intial load carrying capacity (W_{ini}) is depicted for each earthquake.

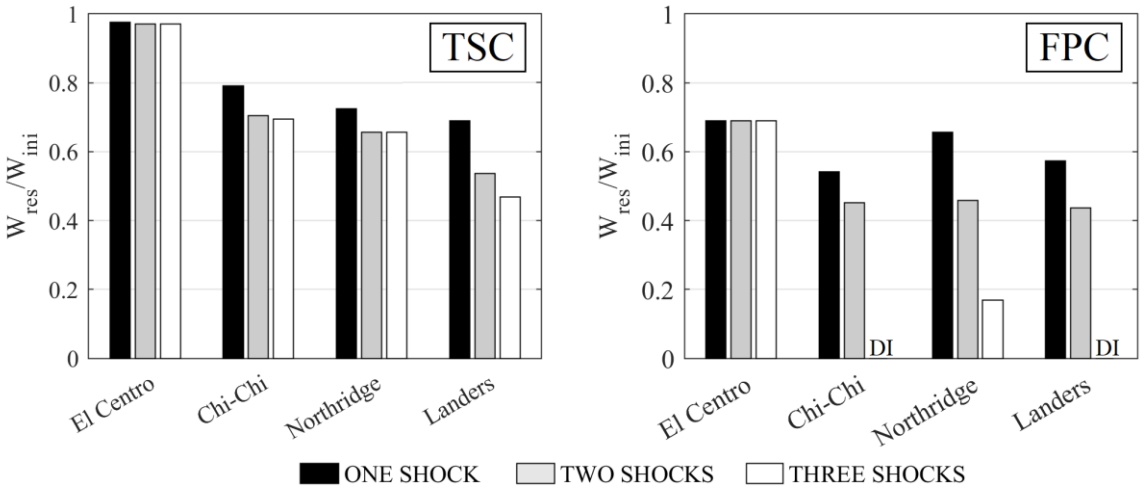

Figure 16 - *Residual load Bearing Capacity and stiffness after each earthquake repetition*

It can be noted that there is a qualitative correlation between the residual load carrying capacity and the residual drift cumulation process. In fact, when structural adaptation occurs, no relevant reduction in the load carrying capacity is observed, as in case of El Centro earthquake. In general, also for this case, low residual load carrying capacity is in FPC frame, whit a reduction is up to 81%, evaluated after the third Northridge repetition. In TSC frame the maximum reduction is obtained from the third repetition of Landers earthquake, up to 31%.

Further information can be obtained from Figure 17, where the results of NLSA analysis are reported only for the cases characterized by a progressive load carrying capacity reduction, i.e. Landers and Northridge earthquake for TSC and FPC frame, respectively. In those cases, it can be noted that non-negligible reductions are provided, not only for load carrying capacity but also for the lateral frame stiffness under the considered load condition. More in detail, the reduction of the global stiffnes can be appraised from the slope of the proposed curves and it can be noted that the slope decreases with the number of considered earthquakes. This behaviour is more highlited in FPC frame under Northridge signal.

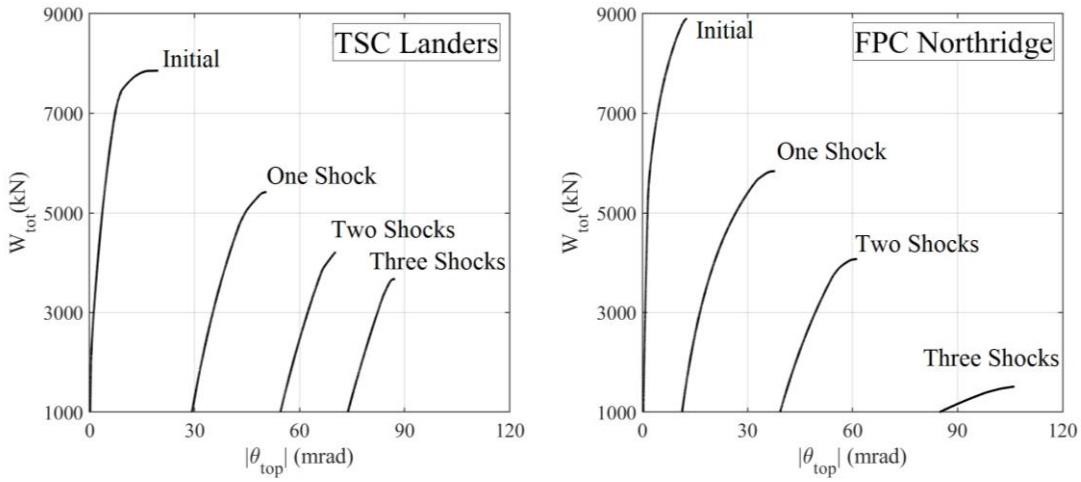

Figure 17 – *Deterioration of load carrying capacity and global frame stiffness, under sequential shocks*

Finally, Figure 18 represents the joint damage value on the Whöler's system after El Centro and Northridge sequential earthquakes, distinguishing the value associated with one, two and three shocks. It is worth noting that, even if in some cases not relevant increments of the residual drift due to further shocks has been observed (as happen in the case of El Centro earthquake), fatigue life is progressively reduced after each earthquake, with the increment of the damage indices.

In case of TSC joints the El Centro damage cumulation trend is quite linear and it can be verified by a lateral translation of the points representing joint damage. A similar trend is provided in case of FPC model under El Centro earthquakes, but in this case the process is not properly linear due to an additional vertical translation of the most damaged zones during the second and the third earthquake. In this case the damage cumulation is slower than in TSC, because the equivalent rotation of joints decreases after each repetition.

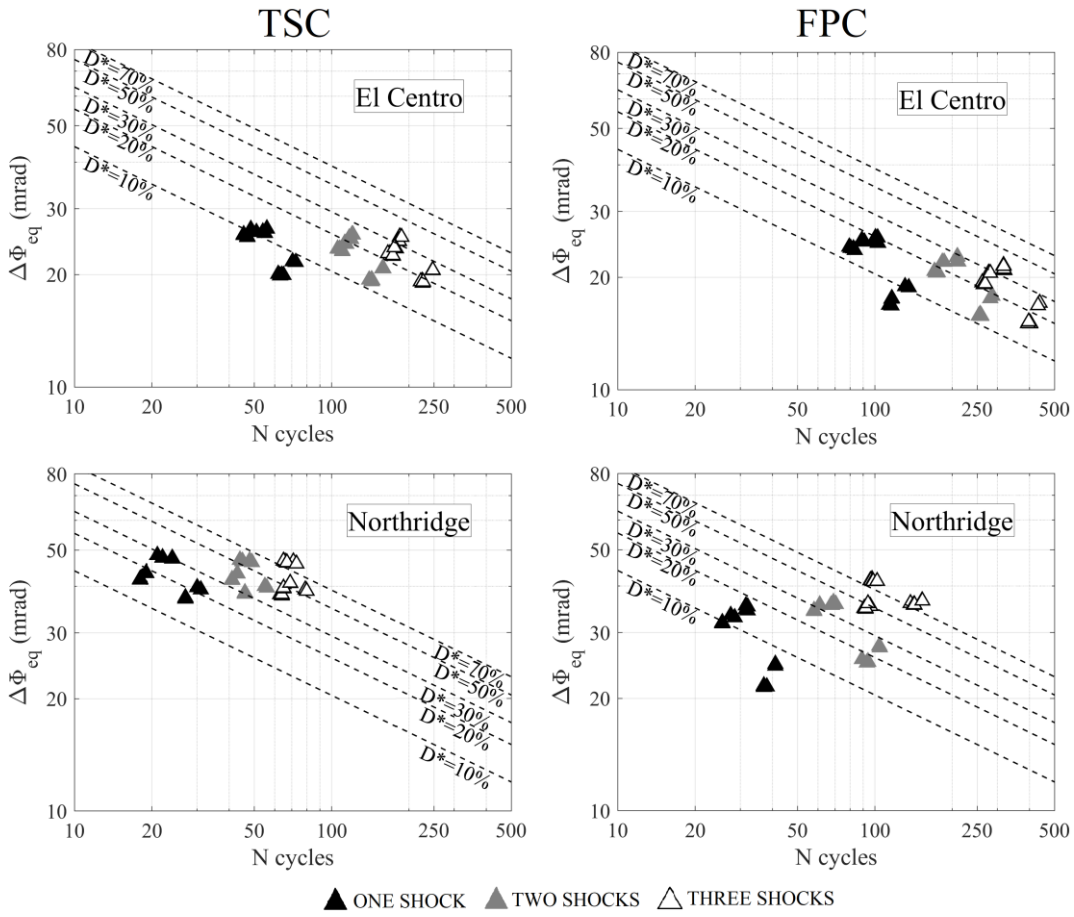

Figure 18 - *Joint damage in sequential earthquake*

When progressive drift accumulation occurs, like in FPC frame during the Northridge earthquake, fatigue cumulation exhibits a non-linear translation in both horizontal and vertical directions, with a relevant increase of the damage indices. For TSC and FPC frame damage indices are quite close to each other for the same earthquake, with the maximum value around 75% after Northridge third repetition and 35% after El Centro.
These results, confirm, also for sequential earthquakes, the remarks associated with a single seismic event. Acceptable performance can be appreciated only in case of TSC frame after El Centro earthquake. In this case, even if local damages linearly increase after each repetition (up to 30%), a stable trend in the residual properties of the structure can be observed, leading to sustainable repair actions. The structure resists to two seismic events even if in most cases, is strongly damaged. Finally, also in the case of the three repetitions, generally the structures survive with high damage, with the exception of FPC frame subjected to both the strongest magnitude earthquakes, were the DI leads to the global collapse.

7 Concluding Remarks

In the paper, a numerical procedure based on a combined application of NLTH analysis and LCF theory has been proposed for the evaluation of the residual performance of MR steel frame structures damaged by one or more earthquakes. After the calibration of the numerical

models with experimental data available in literature, the procedure was applied to two frames differing from beam-to-column joint details and subjected to four different single and sequential earthquakes. Basing on the research outcomes, it is worth noting that:

- fatigue analysis results are strongly influenced by the structural response under a specific ground motion. In particular, large magnitude far field earthquakes are more severe with respect to near field ones;
- the post-earthquake load carrying capacity is greatly influenced by the residual drifts, that are strongly dependent on cyclic joint behaviour;
- no failure is observed in all the cases subjected to a single shock, and the maximum load carrying capacity reduction is up to 39% of the initial value;
- after two sequential shocks, no failure of the frames has been observed despite the relevant values of damage and load carrying capacity reduction;
- structural collapse has been observed only for FPC frame after three Chi-Chi and Landers earthquakes, due to dynamic instability phenomena and not to the achievement of the fatigue life of the steel components.

As a general conclusion, it can be stated that the proposed numerical procedure provides results of relevant importance in the definition of the repairing strategy on a damaged structure. Due to importance of the hysteretic law an accurate calibration of the numerical model is needed. The obtained results should be validated with those detectable during a preliminary inspection phase (i.e. empirical damage index, damage distribution and residual interstorey drifts). Finally, it is worth noting that, due to a limited number of data provided in literature on LCF of steel components extended experimental campaigns could be really useful for extending the application of the proposed procedure to a wider case of connections and steel members.

References

ASTM E1049-85 (2017). Standard Practices for Cycle Counting in Fatigue Analysis. West Conshohocken, PA, ASTM International 2011.

Baggio C., Bernardini A., Colozza R., Corazza L., Della Bella M., Di Pasquale G., Dolce M., Goretti A., Martinelli A., Orsini G., Papa F., Zuccaro J. (2007). Field Manual for post-earthquake damage and safety assessment and short-term countermeasures (AeDES), European Commission Joint Research Centre, Institute for the Protection and Security of the Citizen.

Ballio G., Calado L., Castiglioni C.A. (1997). Low Cycle Fatigue behaviour of structural steel members and connections, Fatigue and Fracture of Engineering Materials and Structures **20(8)**, 1129-1146.

Bannantine J.A., Comer J.J., Handrock J.L. (1989). Fundamentals of Metal Fatigue Analysis, Prentice Hall.

Bernal D. (1992). Instability of Buildings Subjected to Earthquakes. Journal of Structural Engineering **118(8)**, 2239-2260.

Bernuzzi C., Calado L., Castiglioni C.A. (1997). Ductility and load carrying capacity prediction of steel beam-to-column connection under cyclic reversal loading, Journal of Earthquake Engineering **1:2**, 401-432.

Bernuzzi C., Zandonini R., Zanon P (1996). Experimental Analysis and Modelling of Semi-rigid Steel Joints under Cyclic Reversal Loading, Journal of Constructional Steel Research **38(2)**, 95-123.

Bernuzzi C., Chesi C., Rodigari D., De Col R. (2018). Remarks on the approaches for seismic design of Moment Resisting Steel Frames. Ingegneria Sismica - International Journal of Earthquake Engineering **35(2)**, 37-47.

Bernuzzi C., Cordova B., Simoncelli M. (2015). Unbraced steel frame design according to EC3 and AISC provisions. Journal of Constructional Steel Research **114**, 157-177.

Bernuzzi C., Simoncelli M. (2016). An advanced design procedure for the safe use of steel storage pallet racks in seismic zones. Thin-walled Structures **109**, 73-87.

Chiou B., Darragh R., Gregor N., Silva W. (2008). NGA Project Strong-Motion Database. Earthquake Spectra **24(1)**, 23-44.

Clough R., Penzien J. (2003). Dynamics of Structures. Computer and Structures Inc.

Dell'Aglio, G., Montuori, R., Nastri, E., Piluso, V. (2019). Consideration of second-order effects on plastic design of steel moment resisting frames, Bulletin of Earthquake Engineering **17(6)**, 3041-3070.

Dell'Aglio G., Montuori R., Nastri E., Piluso V. (2017). A critical review of plastic design approaches for failure mode control of steel moment resisting frames. Ingegneria Sismica - International Journal of Earthquake Engineering **34(4)**, 82-102.

Denavit M.D., Hajjar J. (2013). Description of geometric nonlinearity for beam column in OpenSees, Department of Civil and Environmental Engineering Reports. Report No. NEU-CEE-2013-02. Department of Civil and Environmental Engineering, Northeastern University, Boston, Massachusetts.

ECCS Technical Committee TC 13 (1994). ECCS Manual on Design of Steel Structures in Seismic Zones, First Edition.

EN 1993-1-1, (2005). Eurocode 3: Design of steel structures – Part 1-1: General rules and rules for buildings, European Committee for Standardization, Brussels.

EN 1993-1-9 (2009). Eurocode 3: Design of steel structures – Part 1.9: Fatigue, EU Committe for standardization.

EN 1998-1, (2004). Eurocode 8: Design of structures for earthquake resistance – Part 1: General rules, seismic actions and rules for buildings, European Committee for Standardization, Brussels.

EN 1998-3, (2005). Eurocode 8: Design of structures for earthquake resistance – Part 3: Assessment and retrofitting of Building, European Committee for Standardization, Brussels.

Ferraioli, M., Lavino, A., Mandara, A. (2018). Effectiveness of multi-mode pushover analysis procedure for the estimation of seismic demands of steel moment frames, Ingegneria Sismica **35(2)**, 78-90.

FEMA 352 (2000). Federal Emergency Management Agency, Recommended Postearthquake Evaluation and Repair Criteria for Welded Steel Moment-Frame Buildings.

FEMA P-58 (2018). Federal Emergency Management Agency, Seismic Performance Assessment of Buildings.

Gioucu V., Mazzolani F.M. (2014). Seismic Design of Steel Structures, CRC Press.

Ibarra L.F., Medina R.A., Krawinkler H. (2005). Hysteretic models that incorporate strength and stiffness deterioration, Earthquake Engineering and Structural Dynamics **34**, 1489-1511.

Kato B. et al. (1997). Kobe earthquake damage steel moment connections and suggested improvements. Japanese Society of Steel construction, Tech. Rep. 39.

Lowes L.N., Mitra N., Altoontash A. (2004). A Beam-Column Joint Model for Simulating the Earthquake Response of Reinforced Concrete Frames, PEER Report 2003/10, Pacific Earthquake Research Center, College of Engineering, University of California, Berkley.

Matsuichi M., Endo T. (1968). Fatigue of metals subjected to varying stress.

Mahin S.A. (1998). Lessons from damage to steel building during the Northridge Earthquake. Engineering Structures **20(4-6)**, 261-270.

McKenna F. (2011). OpenSees: A Framework for Earthquake Engineering Simulation. Computing in Science and Engineering **13**, 58-66.

Miner M.A. (1945). Cumulative damage in fatigue. Journal of Applied Mechanics **12(3)**, A159-A156.

Montuori R., Nastri E., Piluso V., Troisi M. (2016). Influence of the cyclic behaviour of beam-to-column connection on the seismic response of regular steel frames. Ingegneria Sismica - International Journal of Earthquake Engineering **33(1-2)**, 91-105.

Ohi K., Takanashi K. (1998). Seismic diagnosis for rehabilitation and upgrading of steel gymnasium, Engineering Structures **20(4-6)**, 533-539.

Piluso, V., Pisapia, A., Castaldo, P., Nastri, E. (2019). Probabilistic Theory of Plastic Mechanism Control for Steel Moment Resisting Frames, Structural Safety **76**, 95-107.

Rodigari (2020). Earthquake Damage Assessment in Moment Resisting Steel Frames. PhD thesis, Department of Architecture, Built Environment and Construction Engineering, Politecnico di Milano, Italy.

Tartaglia, R., D'Aniello, M., Di Lorenzo, G., De Martino, A. (2018). Influence of EC8 rules on p-delta effects on the design and response of steel MRF, Ingegneria Sismica **35(3)**, 104-120.

Vayas I., Sophocleous A., Dinu F. (2003). Fatigue Analysis of Moment Resisting Steel Frames, Journal of Earthquake Engineering **7**, 635-654.

Youssef N., Bonowitz D., Gross J. (1995). A survey of steel moment resisting frame buildings affected by the 1994 Northridge Earthquake. Report No. NISTIR 5625, Gaithersburg, MD.

Zereian F., Medina R.A. (2010). A practical method for proper modelling structural damping in inelastic plane structural systems, Computers and Structures, Vol. 88, No. p.p.45.33.

ingegneria sismica
International Journal of Earthquake Engineering
Anno XXXVI – Num.4 - 2019

VALUTAZIONE DEL DANNO POST-SISMA DI STRUTTURE METALLICHE INTELAIATE

Claudio Bernuzzi, Davide Rodigari, Marco Simoncelli

Dipartimento di Architettura, Ingegneria delle Costruzioni e Ambiente Costruito
Politecnico di Milano

SUMMARY: *La valutazione del danno nelle strutture che hanno subito uno o più terremoti è di fondamentale importanza per comprendere appieno l'effettivo comportamento post-sisma ed eventualmente, definire le strategie d'intervento più appropriate per l'adeguamento e la riparazione. L'articolo, incentrato sullo studio di telai in acciaio con attacco a momento (MR), si occupa della valutazione post-sisma, dopo uno o più eventi sismici. Una procedura che combina l'analisi sismica dinamica non-lineare agli elementi finiti con la teoria della fatica oligociclica è applicata nella valutazione del danno di ogni componente dei telai analizzati, mentre la capacità portante residua viene calcolata mediante analisi statica incrementale dei telai danneggiati. Dai risultati della ricerca emerge che i calcoli del danno e della capacità portante residua, spesso trascurati nella pratica progettuale, appaiono molto utili nell'aumentare le conoscenze sull'effettivo livello di sicurezza della struttura dopo uno o più sisma.*

KEYWORDS: *strutture intelaiate in acciaio; analisi dinamica non lineare; fatica oligociclica; comportamento ciclico delle connessioni.*

Corresponding author: Marco Simoncelli, Politecnico di Milano, Italy.
Email: marco.simoncelli@polimi.it